

Response to Referee #1 (R1):

In this paper authors present a new dataset of the carbonates system, called SOCOML (Southern Ocean CO₂ Machine Learning), derived from shipboard (GLODAP) and float (Argo) data in the Southern Ocean (here south of 30°S). This is a climatological product that includes aragonite saturation state (Ω_{ar}) and anthropogenic CO₂ concentrations (Cant) for a reference year (2013). Such climatology (for DIC and TA) has been previously developed, based on shipboard data (e.g., Lauvset et al, 2016; Keppler et al 2020, 2023). Like for surface pCO₂ and air-sea CO₂ fluxes products (e.g. SOCOM project, Rödenbeck et al, 2015) successfully used to constraint the estimate of the global carbon budget (Friedlingstein et al, 2025) it is important that different climatology for the ocean interior are available for the community (see also a list of such products in Jiang et al, 2025).

After a clear introduction, authors describe the methodology and uncertainties. Three gridded products are offered (with or without O₂) at 1x1 degree resolution and 84 levels in the water column down to the abyssal domain. This is especially important in the Southern Ocean where AABW are formed and contain significant Cant concentrations (e.g. Rios et al, 2012; Pardo et al, 2017; Mahieu et al, 2020; Zhang et al 2023). This is also challenging as previous analyses explored the changes of Cant inventories over 0-3000m (Gruber et al, 2019; Müller et al, 2023). Here the product extend to the bottom.

The reconstructed fields for AT, DIC, O₂ and nutrients are used to calculate Ω_{ar} and Cant concentrations (here derived from TrOCA method). I suspect this new data-sets could be easily used to estimate Cant using other methods. The results (climatology of TA, DIC, and Cant concentrations) are also important to validate OBGCM and ESM models that suffer to reproduce seasonal to multi-decadal DIC and Cant variability. The results will be also probably useful for paleo-oceanography studies (e.g. using pre-industrial DIC profiles deduced from the data presented in this work when calculate DIC-Cant).

Interestingly, through a comparison of different results, authors indicate that the bias in DIC and Cant depend on the dataset used for the training, highlighting the need of maintaining regular update of the dataset such as GLODAP. This is especially true in region where data are relatively sparse such as near coastal Antarctica and in the seasonal ice zone during austral winter. By the way, I was wondering how the sea-ice is taken into account in the method (or if it should be taken into account).

Thank you for your positive and constructive summary of our work. The comments are detailed and helpful in preparing the revised manuscript.

Regarding the comment on whether sea ice should be considered: it is indeed an important factor influencing the carbonate system in the Southern Ocean through its modulation of air-sea CO₂ exchange and brine-driven processes. To examine whether sea-ice information should be explicitly included as a predictor in the models, we conducted an exploratory test using the monthly sea-ice concentration (SIC) and sea-ice thickness (SIT) product of Fons et al. (2023) covering 2010–2021. SIC represents

the fractional areal coverage of sea ice, whereas SIT describes its vertical depth. Figure R1 below illustrates that sea ice generally persists along the Antarctic coastal margin up to about 70° S, expanding northward during winter, particularly in the Atlantic Sector where it can reach as far as ~55° S.

Machine-learning framework requires one-to-one matched predictors and targets, we therefore collocated SIC and SIT data with the GLODAPv2.2022 for model training. The seasonal ice zone (SIZ; Fig. a) exhibits SIC and SIT variability, but most cruises were conducted during austral summer (mainly in January). South of 55° S, 77 % of the GLODAP measurements have SIC = 0 and 91 % have missing (NaN) SIT values. This indicates that, although sea ice is physically important, it cannot be meaningfully included as an input variable for most samples, nor can machine learning effectively capture transitions from fully ice-covered (SIC \approx 100 %) to open-ocean (SIC \approx 0 %) conditions.

Nevertheless, we conducted preliminary machine-learning experiments to evaluate this possibility. In previous work (Carter et al., 2021), separate neural networks were trained for the Atlantic–Mediterranean–Arctic and Indo–Pacific–Southern sectors to ensure regional representativeness. Within this domain, however, 80–90 % of measured values were associated with missing SIC/SIT data, and even when available, the variability was small—rendering the inclusion of SIC/SIT as predictors ineffective.

To maximize the available samples, we applied monthly SIT fields at each location (month-matched), which yielded a collocated dataset of 47,913 pairs within the SIZ. Among these, approximately 51 % and 32 % contained measured DIC and TA, respectively. We then trained prototype ESPER_NN models using 85% of the collocated dataset for training and 15% for validation, with temperature, salinity, oxygen, and SIC/SIT as predictors and DIC as the target variable. The models did not achieve satisfactory performance: the R^2 remained low regardless of whether sea-ice information was included. This weak performance likely results from the limited measurements south of 60° S, which is insufficient to support robust regional training. Moreover, since the predictors and targets are three-dimensional (longitude, latitude, pressure/depth), whereas SIC/SIT is two-dimensional (longitude, latitude), only about 1,880 unique SIT values provided independent information after accounting for repeated depths.

Physically, sea ice primarily affects the surface and upper mixed layer by air–sea exchange and altering brine processes. Its influence on deeper waters is indirect and occurs mainly through processes associated with the formation of Antarctic Bottom Water (AABW). Based on the spatial distribution of sea-ice cover, this influence is expected to be exerted primarily through AABW formation regions. However, because our product targets the full water column of entire Southern Ocean, the overall impact of sea-ice processes on the deeper ocean interior remains limited. Given the sparse

sampling in ice-covered region and the limited vertical representativeness of sea-ice data, we therefore did not include it as an explicit predictor.

Nevertheless, incorporating sea-ice information is highly relevant for studies focusing on the Antarctic coastal ocean and for reconstructions of surface-ocean properties such as $p\text{CO}_2$ and chlorophyll, which differ in focus from our dataset that targets the broader Southern Ocean interior.

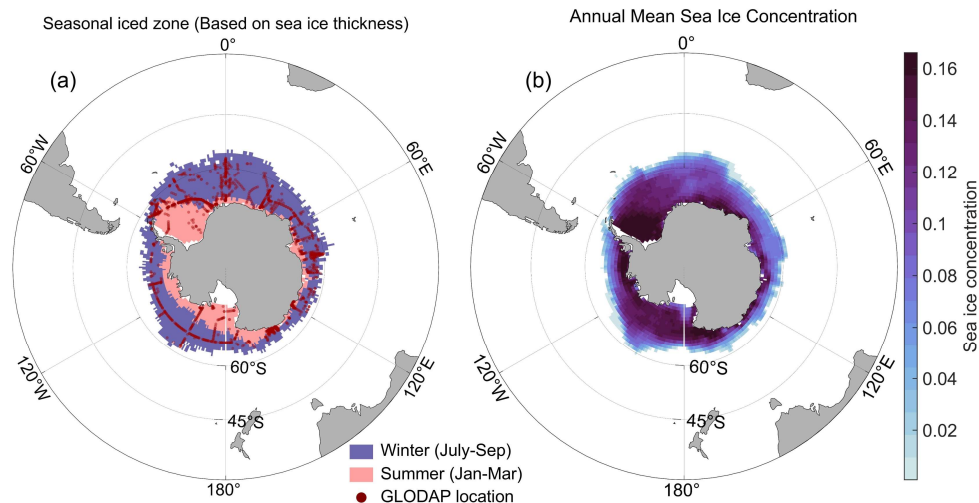


Figure R1. Distribution of sea-ice extent and concentration in the Southern Ocean. (a) Seasonal iced zones derived from sea-ice thickness climatology. Red dots indicate locations of GLODAPv2 observations used in this study. (b) Annual mean sea-ice concentration averaged over 2010–2021.

Fons, S., Kurtz, N., and Bagnardi, M.: A decade-plus of Antarctic sea ice thickness and volume estimates from CryoSat-2 using a physical model and waveform fitting, *The Cryosphere*, 17, 2487-2508, 10.5194/tc-17-2487-2023, 2023.

The manuscript is clear, tables and figures adapted. The dataset will be certainly useful for many studies including validation of models. I recommend publication after some clarifications. Below are listed specific and minor comments.

We sincerely thank the reviewer for the positive and encouraging evaluation. We have carefully addressed all specific and minor comments point by point. The line numbers mentioned in our responses refer to the revised version with *Track Changes* enabled for review.

;;;;;; Specific comments:

C-01: Title: “High-resolution spatiotemporal fields of Southern Ocean interior carbonate system parameters integrated from float- and ship-based observations”. The products are at spatial scale of 1 x 1 degree (not really high-resolution) for a reference year and include anthropogenic CO₂ (Cant) so I would suggest change the title: “Climatological fields of Southern Ocean interior carbonate system parameters and anthropogenic CO₂ integrated from float- and ship-based observations”.

Thank you for your valuable suggestions. Following your recommendation, and in line with Reviewer 2's comment, we have revised the title to:

“Climatological fields of Southern Ocean interior carbonate system parameters and anthropogenic CO₂ reconstructed and integrated from float- and ship-based observations”.

C-02: Line 68: « while the Global Ocean Data Analysis Project version 2 (GLODAPv2, Olsen et al., 2016) offers quality-controlled data product from the surface into the ocean interior includes TA and DIC.” It also offered climatology of TA, DIC in the interior ocean (Lauvset et al, 2016).

Thank you for pointing this out and we have now updated the description to the sentence (Line 68).

“..., while the Global Ocean Data Analysis Project version 2 (GLODAPv2, Olsen et al., 2016) offers quality-controlled data as well as climatological products (Lauvset et al, 2016) from the surface into the ocean interior, including TA and DIC.”

C-03: Line 70: Maybe also refer here to the last RECCAP-2 story for the SO (Hauck et al, 2023).

We have now added the reference of Hauck et al, 2023 (Line 71).

C-04: Line 99: “TA, DIC, pH (total scale), nitrate (NO₃), phosphate (PO₄) and silicate (SiO₄) are obtained through neural networks”. Add also O₂ in this list as this is used for Cant calculation ?

We have now included O₂ in the list and clarified that it is only estimated when direct measurements are not available. The revised sentence now reads (Line 102):

“TA, DIC, pH (total scale), nitrate (NO₃), phosphate (PO₄), silicate (SiO₄), and O₂ (when direct measurements are unavailable) are obtained through neural networks...”

C-05: Line 100-101: « And Cant is estimated using TrOCA method (refs doing the same with TrOCA in Sothern Ocean). » Missing words and references in the sentence ? Also typo: Southern Ocean.

We have added the missing reference (Zhang et al., 2023 and Metzl et al., 2024) and corrected the typo.

C-06: Line 110: Authors used GLODAPv2 data (version GLODAPv2.2020). Are you selecting all the TA and DIC data or only samples when nutrients are all available (Nitrates, silicates and phosphates), i.e. samples without phosphates not included. Also, are you using samples with only TA data or with only DIC data ? Please clarify.

We apologize for the confusion caused by our previous wording. In the revised manuscript, we specify that the data version used is GLODAPv2.2023, to incorporate as many ship-based observations as possible.

It should be clarified that the GLODAP versions used to train the reconstruction models for TA, DIC, pH, and nutrients differ. To enable consistent comparisons in the Southern Ocean, and in particular to evaluate potential effects of temporal trends on model performance, we additionally employed GLODAPv2.2020. The new records included in GLODAPv2.2023 compared to GLODAPv2.2020 were not used in any model training, and thus served as an independent assessment dataset (Table 1) to evaluate model accuracy. In contrast, the Total data listed in Table 1 were used to generate the gridded climatological fields. This explanation also addresses the concern raised in C-15, which we discuss further below.

Regarding the reviewer's question on the use of TA and DIC data: after quality control, we retained TA and DIC samples only when concurrent nutrient measurements (nitrate, phosphate, and silicate) were available, following Carter et al. (2021a). To avoid ambiguity, the text has been revised (Lines 122) as follows:

“Importantly, quality control is performed independently for each variable. Subsequently, TA and DIC measurements are retained only when nutrient observations are available, following Carter et al. (2021a).”

C-07: Line 130: Table 1: maybe specify in the caption that data used are in the SO south of 30°S.

Agreed – added in the caption (Line 135).

C-08: Line 158: “...direct nitrate and pH measurements from Argo floats are excluded from this study.” If I understand authors did not used pH and nitrates data from BGC-Argo floats and used only T, S and O₂ from these floats (correct ?). Please clarify. Maybe a table (as Table 1 for GLODAP) would help to know the final selection of data from floats.

Your understanding is correct. To clarify, we have revised the sentence as:

“...nitrate and pH measurements from BGC-Argo floats are not used in this study; only temperature, salinity, and O₂ are employed.” (Line 164)

In addition, we have added the statistics of Argo float profiles to Table 1 and revised the caption accordingly, as shown below (Line 135):

Table 1. Numbers of shipboard GLODAPv2 measurements and Argo float profiles for each variable in the Southern Ocean used in this study. The assessment dataset of GLODAPv2 data product used for mode-performance comparisons contains cruises added after the GLODAPv2.2020 release—specifically, those with cruise identifiers ≥ 2107 .

	Variables	Oxygen (Y/N)	Assessment dataset	Total
Shipboard GLODAPv2 measurements	TA	N	15,059	103,140
		Y	14,954	101,870
	DIC	N	15,376	129,799

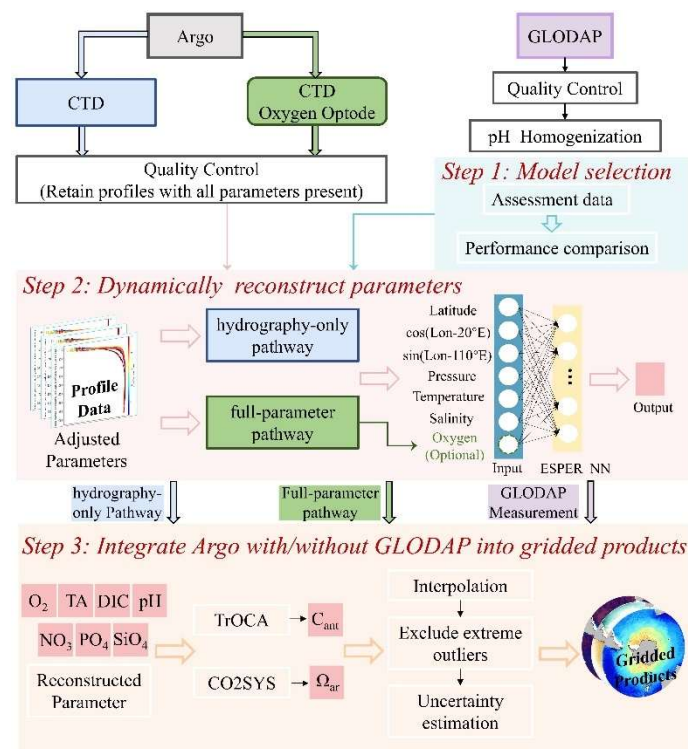
		Y	15,270	126,312
pH		N	14,996	56,597
		Y	14,894	56,411
NO ₃		N	18,796	232,771
		Y	18,575	226,665
PO ₄		N	18,352	224,262
		Y	18,086	218,876
SiO ₄		N	19,011	242,736
		Y	18,745	234,807
Argo float	Temp, Sal	-	-	647,650
profiles	Temp, Sal, Oxy	-	-	73,296

C-09: Line 168: typo CDT: ...blue for Argo only with CTD,

Corrected (Line 172).

C-10: Line 185: Figure 2: In the Box “Step 3”, add O2 in the list of parameters as O2 is used in TrOCA.

We have updated the Figure 2 (Line 190):



C-11: Line 200: Authors used the TrOCA method to derive Cant concentrations that has been successfully used and/or compared in the SO (e.g. Lo Monaco et al, 2005; Vazquez-Rodriguez et al, 2009; Mahieu et al, 2020; Metzl et al, 2024). Authors refer to Lo Monaco et al (2005) but this is not the correct reference for TrOCA (see reference

below). Maybe recall that method is not adapted to estimate C_{ant} in surface layer. How to you extrapolate the C_{ant} concentrations in surface or indicate that climatology is limited to 100m ?

1) The reference to Lo Monaco et al., 2005 has been corrected, and the additional references suggested have been incorporated. The revised sentence now reads:

“For these reasons, this study employs the TrOCA method, which is relatively straightforward, extensively utilized in Southern Ocean studies (Metzl et al., 2024; Zhang et al., 2023), and has been demonstrated to be reliable through comparative analyses (Lo Monaco et al., 2005; Mahieu et al., 2020; Vázquez-Rodríguez; Zhang et al., 2023).” (Line 205)

2) With respect to the concern on surface values, we clarify that the calculation of C_{ant} is limited to waters below the euphotic layer (about 100 m). This restriction has been explicitly added in Section 3.2 and in the dataset metadata. The clarification reads:

“It should be noted that the TrOCA approach is limited to waters below the euphotic layer, therefore the C_{ant} estimates above 100 m are excluded from this dataset.” (Line 212)

C-12: Line 204: “Finally, the C_{ant} values are scaled to the reference year”. It would be useful to specify the reference year, here 2013.

We appreciate the suggestion. We have now specified it here. (Line 210)

C-13: For C_{ant} did you get any negative value?

We acknowledge that this point was not clearly explained earlier. A small number of negative C_{ant} values were identified, which account for only 0.003 % of all samples and appear in about 1 % of the total profiles. An example of an Argo float showing negative values is displayed in the figure below. These negative estimates most likely result from the propagation of methodological and observational uncertainties. It is worth noting that the mean of all negative values is $-1.08 \mu\text{mol kg}^{-1}$, and their deviation from zero generally falls within the estimated uncertainty range of C_{ant} of approximately $\pm 6 \mu\text{mol/kg}$. Therefore, although negative C_{ant} values are physically unrealistic, they are mathematically reasonable within the context of uncertainty propagation. To ensure consistency in the mathematical treatment of error propagation, we followed the approach of Gruber et al. (1998) and retained these negative C_{ant} values in the averaging process to avoid introducing artificial biases into the gridded fields. To clarify this point, we have added the following sentence to the main text:

“Following Gruber et al., 1998, negative C_{ant} value is preserved in the averaging process.” (Line 242)

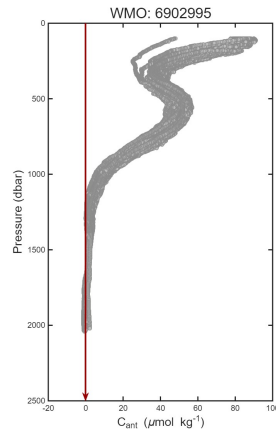


Figure R2. Vertical distribution of anthropogenic carbon (C_{ant}) estimated using Argo float (WMO: 6902995). Each grey dot represents an individual estimate and the red line at zero indicates the reference for distinguishing positive and negative C_{ant} values.

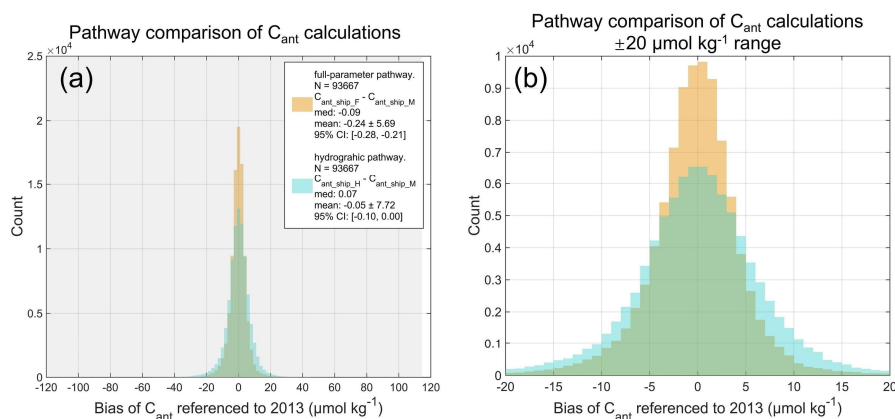
C-14: Line 207: I guess Lewis et al (2021) not listed in references.

Thank you for noticing this oversight. The reference has been corrected and listed: it should be *Sharp et al., 2023* instead of *Lewis et al., 2021*. (Line 214)

Sharp, J. D., Pierrot, D., Humphreys, M. P., Epitalon, J.-M., Orr, J. C., Lewis, E. R., and Wallace, D. W. R.: CO2SYSv3 for MATLAB (Version v3.2.1), Zenodo [code], <https://doi.org/10.5281/zenodo.3950562>, 2023.

C-15: Line 330: “Under the full-parameter pathway, C_{ant} exhibits a slight negative bias relative to shipboard derived values ($C_{ant_ship_M}$),” Curiosity: Is there any change of the bias over time or is it evaluated for the reference year only?

This is an important question. When evaluating the bias of float-derived values relative to shipboard-derived values ($C_{ant_ship_M}$), we initially did not apply normalization. We have now recalculated the normalized bias, and the updated results are shown in the revised Figure 4 (Line 365).



In addition, we examined whether machine-learning reconstructions can capture temporal trends in C_{ant} . A scatterplot of bias versus year (see below) shows no evident trend. It is nevertheless likely that biases may emerge in future years due to the exponential increase in atmospheric CO_2 , particularly in the Southern Ocean where

C_{ant} penetration is more pronounced. However, empirical approaches such as machine learning risk projecting natural variability into apparent long-term trends (Carter et al., 2021), as they are not designed to resolve non-steady-state variations in C_{ant} .

In practice, most machine-learning models are constructed under the assumption that the ocean operates in a steady state. For example, Sauzède et al. (2017) and Bittig et al. (2018) incorporated sampling date information directly into the input parameters, whereas Carter et al. (2021) developed the ESPER model by adjusting DIC and pH values to a reference year before training and then re-adjusting them to the desired year at the output stage. Both approaches rely on the assumption of short-term oceanic steady state within the sampling period of the training data. This methodological constraint limits the use of machine-learning reconstructions to assess trends in the bias of DIC and C_{ant} .

For these reasons, in this study we chose to present climatological distributions of carbonate system parameters and nutrients rather than focus on temporal trends. Nonetheless, we acknowledge that developing approaches for machine learning to better capture long-term trends and potentially seasonal variability remains an important direction for future work.

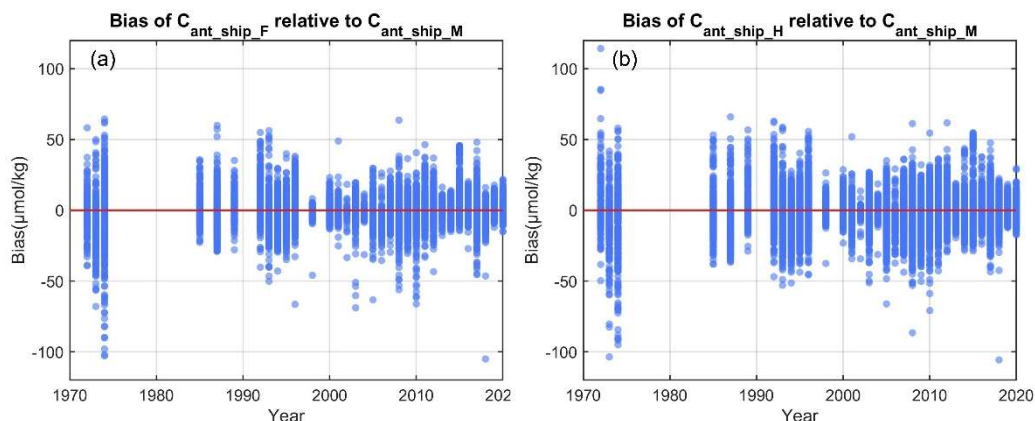


Figure R3. Temporal distribution of biases in C_{ant} estimates.

C-16: Figure 6b: The map is not clear. Is it for surface water, for deep layers? Please clarify in the caption.

Thank you for this observation. The comparisons in Figure 6b are restricted to the 1,400-2,100 dbar depth range. We have clarified this in both the caption (Line 374) and the manuscript text (Line 353).

C-17: Line 364: Climatological distribution. Could you recall the period for the climatology presented in Figure 7 and 8; it is a mean for any data spanning 1972-2025 or for a reference year in 2013 ?

Figure 7 and 8 illustrate the spatial distribution of the Float Grid, as noted in Line 372. The climatology represents a mean of Argo profile data spanning 2001-2024 for TA,

DIC, pH, Ω_{ar} , and nutrients, while C_{ant} is expressed as a mean for a reference year 2013. We have clarified this in the captions of Figure 7, 8, A4, A5, and A6.

C-18: Line 375: when describing the fronts plotted in figure 7 (STF, SAF, PF...), add a reference (Orsi et al 1995, other ?).

A reference to Orsi et al. (1995) has been added when describing the fronts plotted in Figures to provide appropriate citation.

C-19: Figures 7 and 8. I think a map is missing: “Abyssal water” listed in the captions.

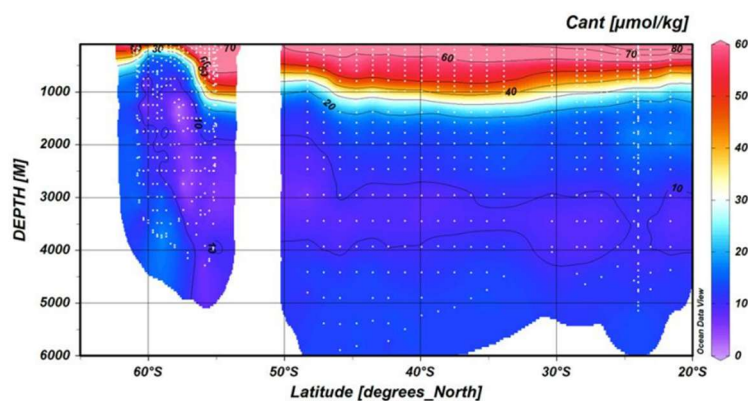
Sorry for our incaution. The caption has been revised, and the abyssal-layer distributions have now been incorporated into the main text, following the related suggestion in Comment C-29.

C-20: Figures 7 and 8. Maybe specify in the caption that the color scales are different for each map.

We have revised the caption by adding the statement “Note that the color scales differ among the individual maps” at the end.

C-21: Figure 7f,g show high C_{ant} in the SW Atlantic ($>20 \mu\text{mol/kg}$?). This signal is not resolved for the O2-Float-grid (Figure 9a). A comment on this ? Is TrOCA not adapted here or a problem with reconstruction? (see also comment C-27 below)?

Figure R1; Section of C_{ant} ($\mu\text{mol/kg}$) along cruises in the South-Western Atlantic (GLODAP data in 2018-2019, Expocode: 29HE20190406 and 74JC20181103). In deep layers, below 1500m, there is no concentration higher than $20 \mu\text{mol/kg}$ as suggested in Figure 7 f,g.



Thank you for prompting us to reconsider this point carefully. Following your comment (see also C-27), we conducted a detailed re-examination of the parameter distributions in the southwestern Atlantic (SW Atlantic; 60°W – 30°W , 30°S – 60°S).

(1) High C_{ant} concentrations ($>20 \mu\text{mol/kg}$)

We first inspected the GLODAP data in this region. As you noted, for the two cruises (Expocode: 29HE20190406 and 74JC20181103), the vertical profiles of C_{ant}

calculated using the TrOCA method (Figure R4a) show no concentrations exceeding $20 \mu\text{mol kg}^{-1}$ in the deep ocean, consistent with your observation. It should be noted that the DIC data of cruise 29HE20190406 south of 30°S have quality flags = 0; therefore, these data were excluded from our DIC and C_{ant} analysis. Figure R4b presents all TrOCA-derived C_{ant} data from GLODAP within the SW Atlantic, revealing a few isolated deep-ocean values above $20 \mu\text{mol kg}^{-1}$. Moreover, Zhang et al. (2023) also reported scattered $> 20 \mu\text{mol kg}^{-1}$ values in the deep waters of the Weddell Sea and the adjacent SW Atlantic based on three independent methods for estimating C_{ant} (Figure R5), suggesting that the TrOCA approach remains applicable in this region.

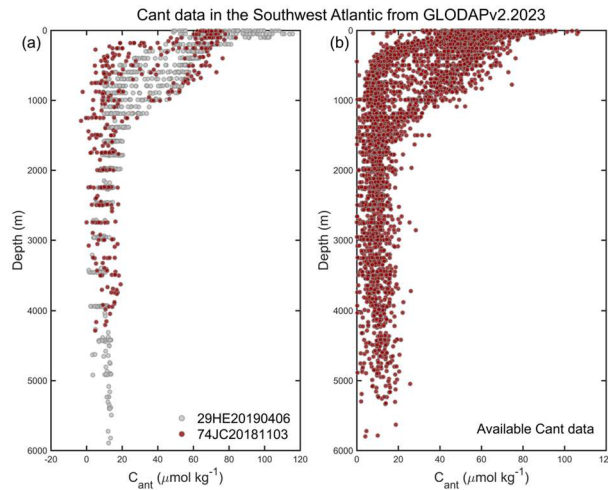


Figure R4. Vertical distribution of C_{ant} in the southwest Atlantic from GLODAPv2.2023.

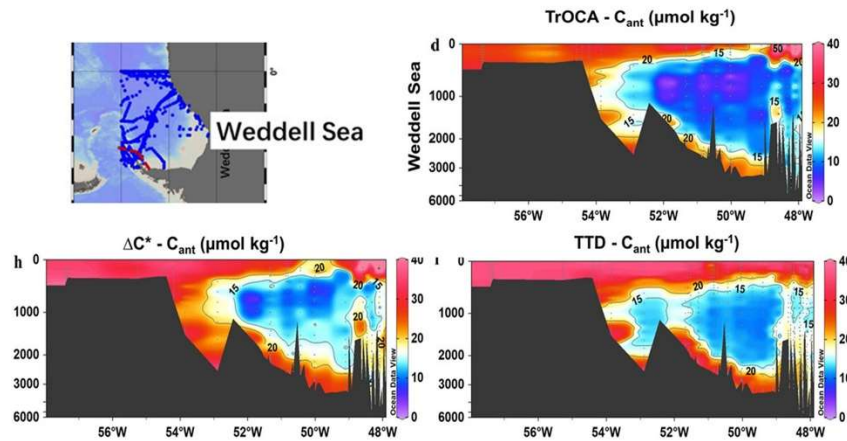


Figure R5. Comparison of C_{ant} estimates in the SW Atlantic Ocean near Weddell Sea (Zhang et al., 2023).

(2) Difference between O2-Float Grid and non-O2-Float Grid

Temperature and salinity profiles from Core and BGC Argo floats are generally consistent, and the distributions of dissolved oxygen measured by BGC Argo floats agree well with those reconstructed from Core Argo data (Figure B3), confirming that the O_2 reconstruction in this region is reliable. However, the profiles of TA, DIC, and consequently C_{ant} and Ω_{ar} exhibit noticeable differences (Figures B4), arising from the

inherent limitations of the machine-learning model that lead to distinct reconstruction pathways.

In Section 4.2, we analyzed in detail how the two reconstruction pathways influence C_{ant} and Ω_{ar} based on shipboard measurements. We further assessed these pathway differences using float data located near the shipboard sites, focusing on a restricted depth range (1,400–2,100 dbar) and comparable seawater property conditions. From this joint analysis of GLODAP and float data, we found that the differences in float-based C_{ant} and Ω_{ar} between the two pathways are within $\pm 10 \mu\text{mol kg}^{-1}$ and ± 0.075 unit, respectively.

However, in regions with sparse training data—such as the SW Atlantic—our gridded product exhibits noticeably larger discrepancies between the O_2 -Float and non- O_2 -Float Grid products. This reflects a common limitation of neural-network and other regression-based methods. To quantify this, we used BGC-Argo floats carrying O_2 sensors to compare the hydrography-only pathway (T, S) against the full-parameter pathway (T, S, O_2). For each $1^\circ \times 1^\circ$ bin, we calculated the mean vertical difference in C_{ant} and Ω_{ar} between the two pathways, and the resulting distribution is shown in Figure B2. As the full-parameter pathway includes observed O_2 and thus yields more constrained results, we consider its reconstructed C_{ant} and Ω_{ar} to be more accurate. The comparison reveals a clear overestimation of C_{ant} and localized underestimation of Ω_{ar} in the SW Atlantic under the *hydrography-only* pathway. Similar but weaker differences are observed near the Ross Sea (overestimated C_{ant} , underestimated Ω_{ar}) and along the Pacific coast of South America (underestimated C_{ant} , overestimated Ω_{ar}), although their spatial patterns are much less pronounced. The pronounced differences in the SW Atlantic arises from the limited number of shipboard training samples in this region—only about 1.3 % of the quality-controlled GLODAPv2.2023 measurements in the Southern Ocean contain both TA and DIC measurements. The performance of the machine-learning reconstructions and our gridded dataset is expected to improve as more such high-quality data become available in this area. In the SW Atlantic, C_{ant} exhibits a more stratified vertical structure rather than the deep-penetrating signal captured by the non- O_2 -Float grid. Therefore, for studies focused on specific regions such as the SW Atlantic, we recommend using the O_2 -Float Grid provided in this study.

(3) Revision in the main text

Accordingly, we have revised the relevant section in the manuscript to clarify this issue and have added a brief discussion on the regional limitation of the reconstruction pathways in the SW Atlantic in Appendix B.

a. Appendix B2. Differences between reconstruction pathways for float-based products

“To quantify the differences between the two reconstruction pathways of Argo floats, BGC-Argo floats equipped with O_2 sensors are used to compare the hydrography-only pathway with the full-parameter pathway. For each $1^\circ \times 1^\circ$ grid cell, the averaged

vertical difference in C_{ant} and Ω_{ar} between the two pathways are calculated (Figure B2). Because the full-parameter pathway incorporates measured O_2 and therefore provides better-constrained results, its reconstructions of C_{ant} and Ω_{ar} are regarded as more accurate. The comparison reveals a clear overestimation of C_{ant} and a localized underestimation of Ω_{ar} in the southwestern Atlantic under the hydrography-only pathway. The Ω_{ar} difference primarily occurs within the intermediate layer. Similar but weaker differences are observed near the Ross Sea (overestimated C_{ant} , underestimated Ω_{ar}) and along the Pacific coast of South America (underestimated C_{ant} , overestimated Ω_{ar}), although their spatial patterns are much less pronounced. The pronounced differences in the southwestern Atlantic likely arises from the limited number of shipboard training samples in this region (only about 1.3 % of the quality-controlled GLODAPv2.2023 measurements in the Southern Ocean contain both TA and DIC measurements). The performance of the machine-learning reconstructions and the gridded dataset is expected to improve as additional high-quality data become available.” (Line 592)

b. Appendix B3. Regional profile distribution in the southwestern Atlantic

“From the climatological distribution of C_{ant} and Ω_{ar} in the O_2 -float Grid and non- O_2 -float Grid, a hotspot of high C_{ant} concentrations and low Ω_{ar} appears in the southwestern Atlantic Ocean (SW Atlantic) near the SAF and PF. Temperature and salinity profiles from Core and BGC Argo floats are generally consistent, and the profile distributions of O_2 measured by BGC Argo floats agree well with those reconstructed from Core Argo data (Figure B3), confirming that the O_2 reconstruction in this region is reliable. However, the profiles of TA, DIC, and consequently C_{ant} and Ω_{ar} exhibit noticeable differences (Figures B4), arising from the inherent limitations of the machine-learning model that lead to distinct reconstruction pathways (detailed in Appendix B2). In the SW Atlantic, C_{ant} exhibits a more stratified vertical structure rather than the deep-penetrating signal captured by the non- O_2 -Float grid. For regional studies, particularly in the southwestern Atlantic, we recommend using the O_2 -Float Grid provided in this study.” (Line 610)

c. Revise the main text in Section 4.3

“Figures 7, 8 illustrate the climatological spatial distribution of the interior carbon system parameters of the Float Grid. The spatial patterns of the gridded products are generally consistent, except for C_{ant} and Ω_{ar} in the southwestern Atlantic (shown in Figure B2). To address this issue, the corresponding O_2 -Float Grid distributions are additionally provided. Section 4.4 further provides a detailed comparison among these products and shipboard estimates.” (Line 381)

“Conversely, higher C_{ant} concentrations ($>20 \mu\text{mol kg}^{-1}$) are observed in the Pacific sectors and areas south of the PF in the eastern Antarctic region.” (Line 402)

d. Revise the main text in Section 4.4

“Notably, a hotspot of high C_{ant} and vertically confined low Ω_{ar} is identified in the southwestern Atlantic Ocean near the SAF and PF in the Non-O₂-Float Grid (Figure 10a). These noticeable differences likely arise from the limited number of shipboard training samples in this region, leading to reduced performance of the machine-learning reconstructions. For regional studies in the southwestern Atlantic, we therefore recommend using the O₂-Float Grid provided in this study. The corresponding vertical profiles are presented in Appendix B3. Although float-based measurements introduce additional uncertainties, their extensive spatial and temporal coverage enables our products to offer unprecedented insight into the previously under-sampled Southern Ocean, particularly in the deep ocean.” (Line 457)

e. Revise Figure 7 (Line 415) and 8 (Line 422)

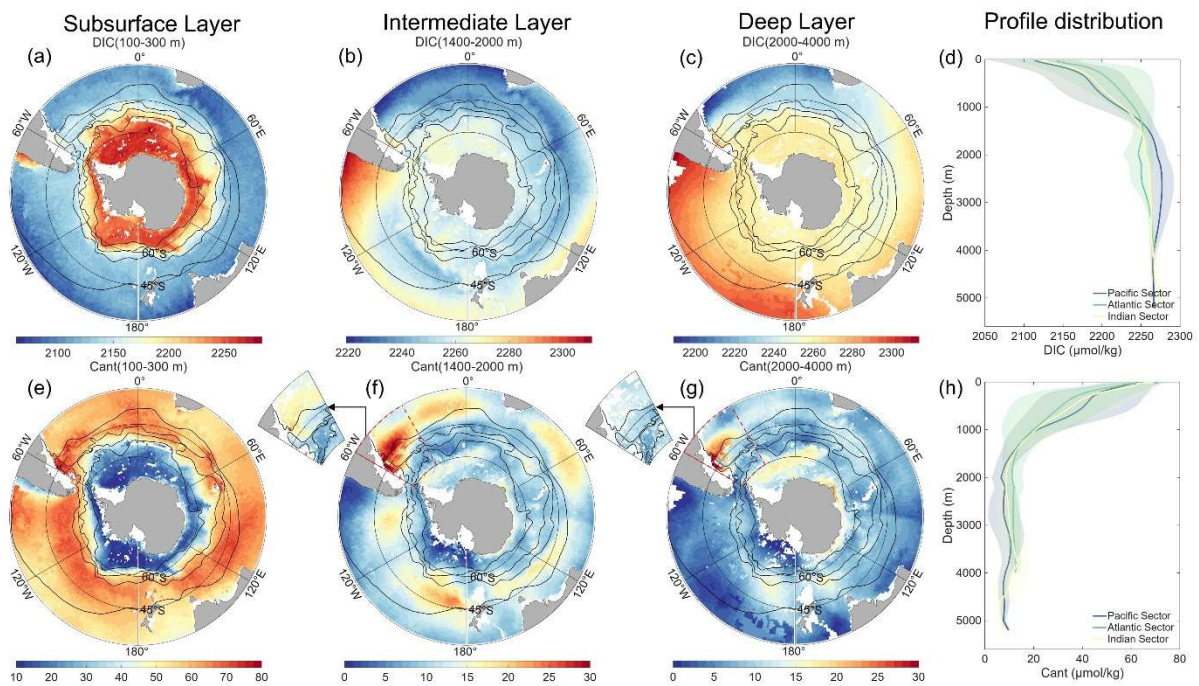


Figure 7. Averaged climatological distribution of DIC (a-d) and C_{ant} (e-h) in oceanic sectors and three layers: subsurface layer (100 to 300 m), intermediate layer (1400 to 2000 m), and deep layer (2000 to 4000 m). The climatology is based on the Float Grid derived from Argo profile data spanning 2001-2024 for DIC, while C_{ant} is scaled to the reference year 2013. In the southwestern Atlantic, where noticeable differences of C_{ant} in deep waters occur between different data products (see explanation in Appendix B2 and B3), the corresponding O₂-Float Grid distributions for the intermediate and deep layers are additionally shown as the inset to the subplot (f, g). The thin black lines show, from north to south, the Subtropical Front (STF), the Subantarctic Front (SAF), the Polar Front (PF), and the Southern Antarctic Circumpolar Current Front (SACCF) (Oris et al., 1995). Note that the color scales differ among the individual maps.

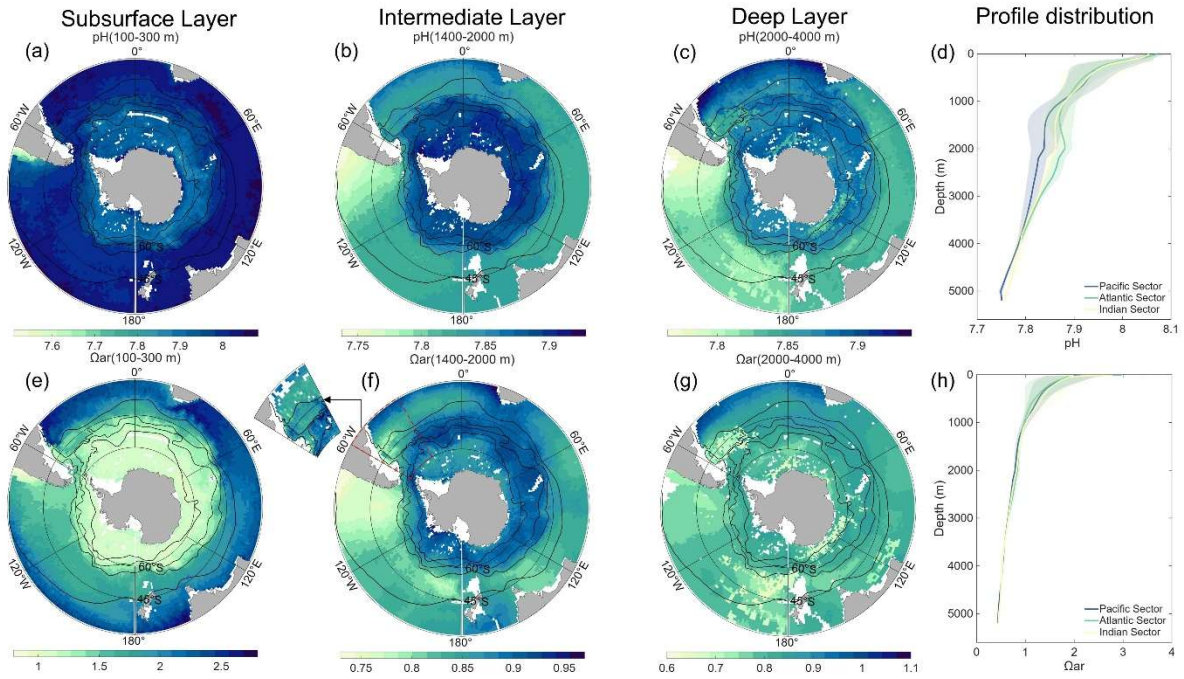


Figure 8. Averaged climatological distribution of pH (a-d) and Ω_{ar} (e-h) in oceanic sectors and three layers: subsurface layer (100 to 300 m), intermediate layer (1400 to 2000 m), and deep layer (2000 to 4000 m). The climatology is based on the Float Grid derived from Argo profile data spanning 2001-2024. In the southwestern Atlantic, where noticeable differences of C_{ant} in deep waters occur between different data products (see explanation in Appendix B2 and B3), the corresponding O_2 -Float Grid distribution for the intermediate layer is additionally shown as the inset to the subplot (f). The thin black lines show, from north to south, the Subtropical Front (STF), the Subantarctic Front (SAF), the Polar Front (PF), and the Southern Antarctic Circumpolar Current Front (SACCF) (Oris et al., 1995). Note that the color scales differ among the individual maps.

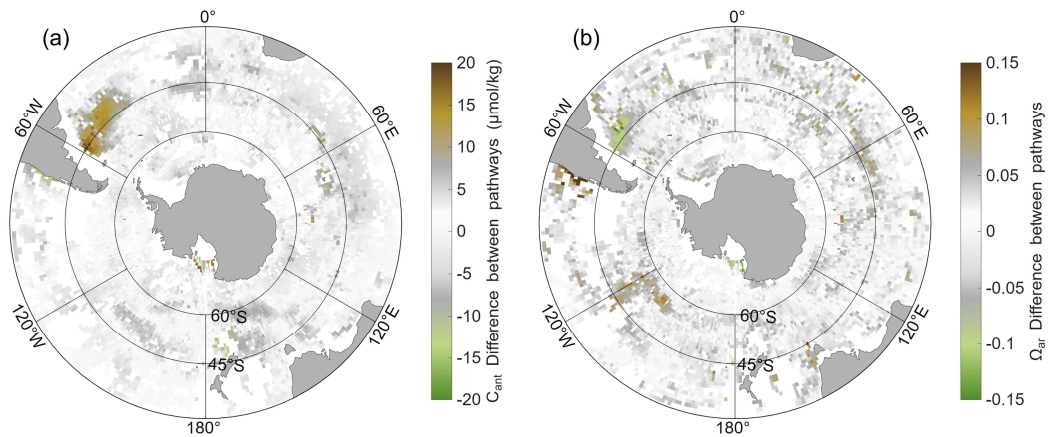


Figure B2. Differences between reconstruction pathways for (a) C_{ant} ($\mu\text{mol kg}^{-1}$) and (b) Ω_{ar} from BGC-Argo floats with O_2 sensors. For each $1^\circ \times 1^\circ$ bin, the mean vertical difference between the hydrography-only and full-parameter pathways are calculated. Values falling within the range derived from float-shipboard matchups are shown in grey, whereas brown and green indicate positive and negative differences, respectively.

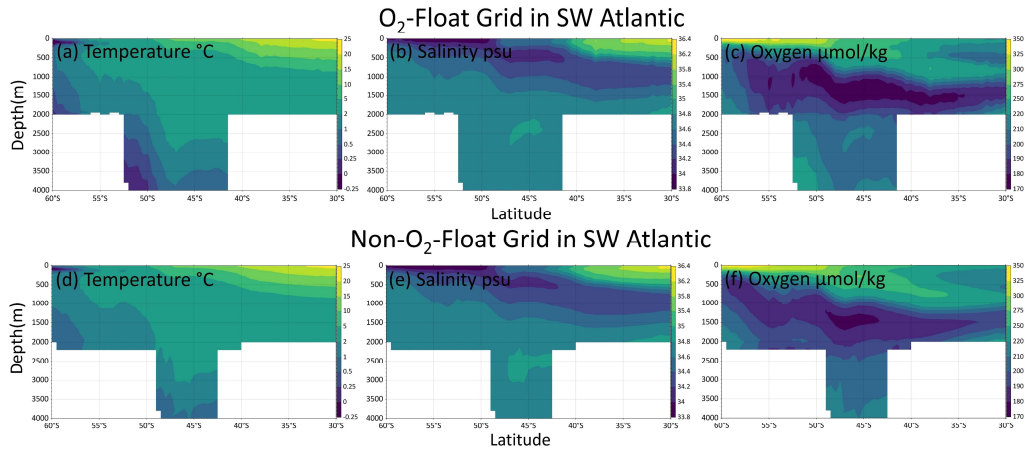


Figure B3. Zonal-mean sections (averaged between 60°W and 30°W) of temperature, salinity, and oxygen from 60°S to 30°S in the southwestern Atlantic Ocean. Panels (a-c) show profiles from the O₂-Float Grid, and panels (d-f) from the Non-O₂-Float Grid. Note that oxygen is measured in panel (c) and reconstructed in panel (f).

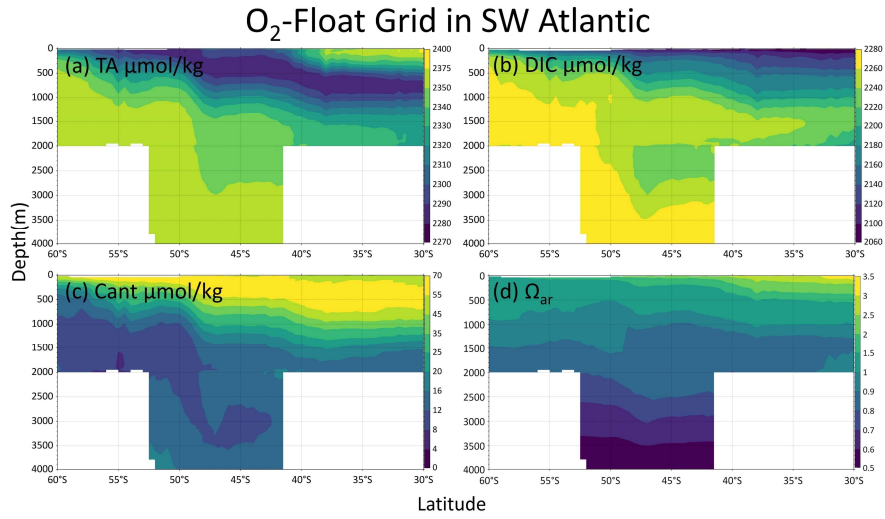


Figure B4. Zonal-mean sections (averaged between 60°W and 30°W) of TA (a), DIC (b), C_{ant} (c), and Ω_{ar} (d) from 60°S to 30°S in the southwestern Atlantic Ocean. The profiles are from the O₂-Float Grid.

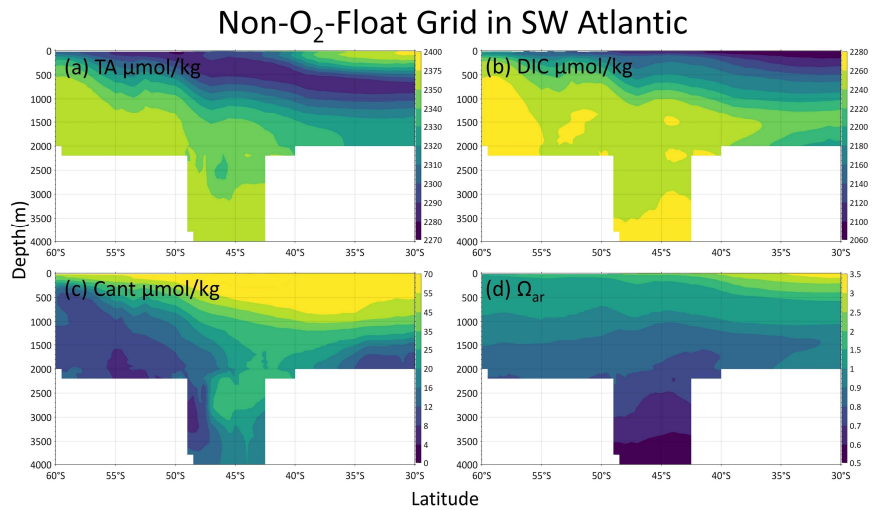


Figure B5. Zonal-mean sections (averaged between 60°W and 30°W) of TA (a), DIC (b), C_{ant} (c), and Ω_{ar} (d) from 60°S to 30°S in the southwestern Atlantic Ocean. The profiles are from the Non-O₂-Float Grid.

C-22: Figures 9a: Few data show very high Cant in the Pacific and Indian oceans (red points apparently > 25 $\mu\text{mol/kg}$). Are the data correct ? The maps 9a and 9c on top (shipboard) are small and it would be nice to show enlarged maps in Supp Mat.

We appreciate this careful observation. Figure 9a is intended to present the climatological distribution of C_{ant} within the 1400–2000 dbar layer (intermediate layer, consistent with Figure 7f). However, we mistakenly indicated a deeper layer in the original caption. This has now been corrected. In addition, enlarged versions of the shipboard-based maps have been added to Figure A9 after consideration of the reviewer's suggestion.

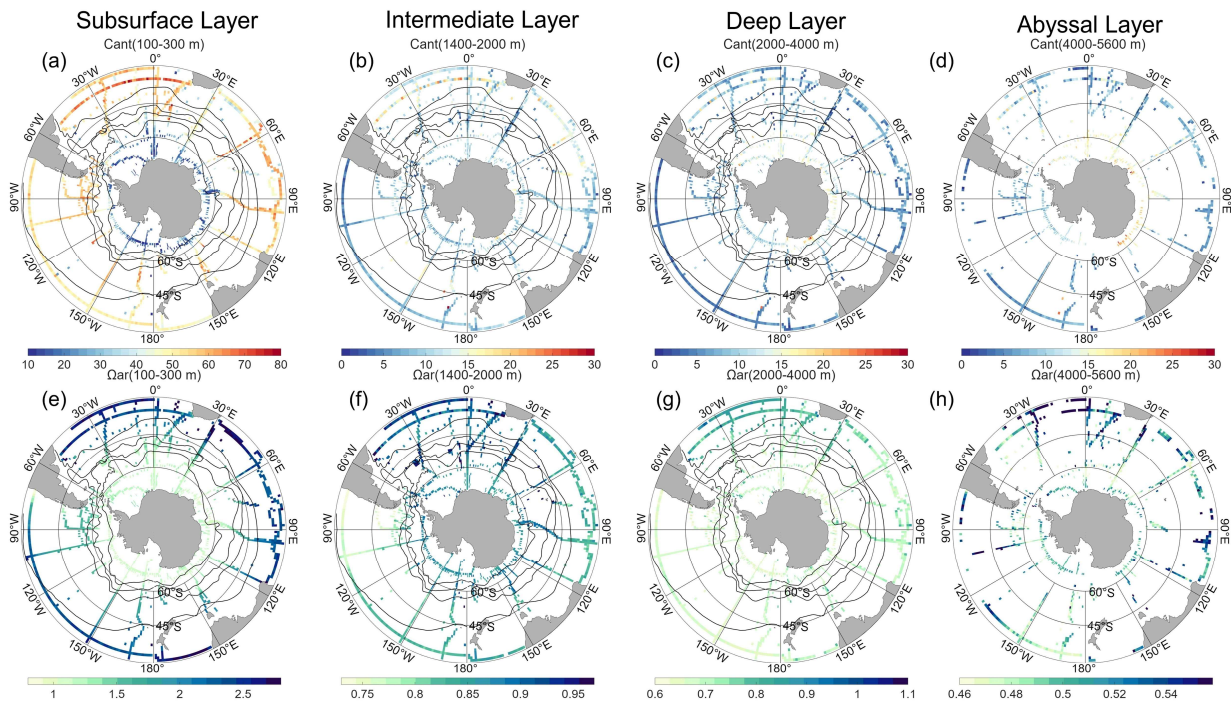


Figure A9. Averaged climatological distribution of C_{ant} (a-d) and Ω_{ar} (e-h) in oceanic sectors and three layers: subsurface layer (100 to 300 m), intermediate layer (1400 to 2000 m), deep layer (2000 to 4000 m), and abyssal layer (4000 to 5600 m). The climatology is derived from GLODAPv2.2023, while C_{ant} is scaled to the reference year 2013. The thin black lines show, from north to south, the Subtropical Front (STF), the Subantarctic Front (SAF), the Polar Front (PF), and the Southern Antarctic Circumpolar Current Front (SACCF) (Oris et al., 1995). Note that the color scales differ among the individual maps.

C-23: Figures 9a and 9c: Could you recall in the caption the layer for the maps in deep layers (2000- 4000 db ?)

The caption has been revised to specify the pressure range of layers.

C-24: Figures 9: the scales at the bottom is not clear (or not fully plotted)

We have revise the color scale of Ω_{ar} and updated in Figure 9 and corresponding Figure 8g.

C-25: Figures 9b: would it be possible to change the color for the lines (not clear for GLODAP: green in legend ?).

We acknowledge the inconsistency in the previous color scheme for GLODAP between the legend and the subsurface panels. We have corrected this issue and replaced the original color with a clearer one to improve visual distinction. Together with the revisions made in response to C-23 and C-24, the figure has been updated accordingly as shown below (Line 470).

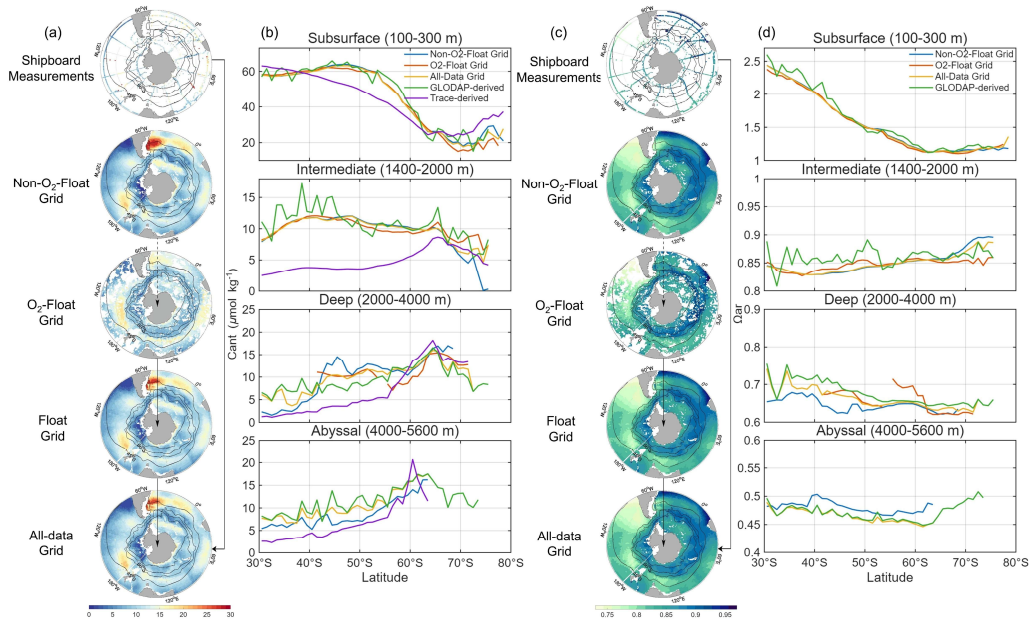


Figure 10. Panels (a) and (c) show the climatological distribution of C_{ant} and Ω_{ar} in the intermediate layers (1400-2000 m), respectively. Panel (b) and (d) present latitudinal distributions of C_{ant} and Ω_{ar} averaged over four depth layers: subsurface layer (100 to 300 m), intermediate layer (1400 to 2000 m), deep layer (2000 to 4000 m), and abyssal layer (4000 to 5600 m). Black, red, blue, green and purple symbols and lines represent Non- O_2 -Float Grid, Float Grid, All-Data Grid, GLODAP-derived data, and TraceV1-derived data, respectively.

C-26: Line 417: “The TRACE-derived dataset (purple lines) consistently underestimates C_{ant} relative to the TrOCA-derived values, particularly in intermediate waters.” WHY ?

We acknowledge that our original wording was misleading. The intention was not to suggest that TRACE underestimates or TrOCA overestimates C_{ant} , but simply to indicate that the TRACE-derived dataset yields lower C_{ant} concentrations than the TrOCA-derived values.

According to Carter et al. (2025), TRACEv1 is essentially an observation-tuned, model-based product in the deep ocean but shows limitations in regions where relatively young waters mix with older deep waters in substantial amounts (e.g., Antarctic Intermediate Water). In such regions, the one-dimensional idealized “pipe model” age distribution used in TRACEv1 is often inadequate, and the simple inverse Gaussian (IG) formulation is limited when reconstructing modelled C_{ant} .

In addition, TRACEv1 tends to exhibit larger reconstruction errors in regions with sparse training data. Because transient tracer measurements that include all three tracers (CFC-11, CFC-12, and SF_6) remain relatively rare—representing only about 5 %

globally of the GLODAPv2.2023 dataset. Our analysis shows that in the Southern Ocean, only 37,258 transient tracer samples are available, with merely ~10 % of them located in intermediate waters. Given the complex water-mass structure and strong upwelling in intermediate layers in 30° S-60° S, the scarcity of tracer observations likely contributes to discrepancies between the model-based TRACEv1 product and our observation-based TrOCA estimates.

We leave this issue for future work. With the continued expansion of seawater property and transient tracer measurements in the Southern Ocean, it will become possible to better evaluate the consistency among different anthropogenic carbon estimation methods and improve both empirical calculations and model simulations.

The corresponding section in the manuscript has been revised as follows:

“Additionally, we apply the TRACE method (Carter et al., 2025) to estimate C_{ant} , generating a gridded dataset as described in Section 3.3, which serves as an additional comparison (Figure 9b). TRACEv1 adopts a hybrid conceptual framework, with surface-ocean estimates that are observation-based, whereas deep-ocean fields are model-based and tuned against observations.” (Line 439)

“The TRACE-derived dataset (purple lines) yields lower C_{ant} concentration than the TrOCA-derived values, particularly in intermediate waters. This difference may partly arise because the model-based approach is difficult to constrain accurately in regions with sparse transient tracer observations and complex vertical structures associated with Southern Ocean upwelling (as suggested by Carter et al., 2025), leading to deviations from the observation-based TrOCA estimates.” (Line.445)

C-27: Line 426: “Notably, we identify a hotspot of high C_{ant} concentrations in the southwestern Atlantic Ocean near the SAF and PF (Figure 9a), potentially linked to AABW outflow from the Weddell Sea”. Intriguing signal (see comment C-21). If the selected depth for Figure 9a is 2000-4000db, would the signal linked to waters above the AABW (e.g. WSDW) or other origin (see for example Gruber, 1998; Ríos et al, 2012). Note also that Müller et al (2023) identified a relatively high increase of the C_{ant} inventory in this region between 2004 and 2014 (for the layer 0-3000m). It would be interesting to show a section of C_{ant} (Lat/depth) crossing this region in the Appendix. See for example figure R1 in this review. Would that anomaly in the SW Atlantic help to check the data or the methods ?

;;;;;; Figure for review

Refer to C21.

C-28: Line 453: “Although our approach may underestimate uncertainty due to potential representativity error, our dataset offers a significant improvement in both accuracy and spatial representativeness over previous gap-filling approaches”. Maybe also recall that your product is extended to the bottom whereas previous analyses were mainly limited to the layer 0-3000m (e.g. Gruber et al, 2019).

Thank you for this insightful suggestion. We have now revised the sentence in Line 479 accordingly and incorporated a brief reference to this point in the Introduction.

In the *Introduction*, we now introduce this aspect as a motivating point:

“In this study, we leverage the ESPER_NN model, integrating the high-accuracy GLODAPv2 database with profiling measurements of fine spatiotemporal resolution, to generate a comprehensive carbonate system dataset throughout the interior Southern Ocean that extends from the surface to the deep ocean (5,600 m).” (Line 99)

C-29: Figure A6: For the abyssal water, the maps are not clear. Why there are so few data. Also change the code for the panels (a), (b), (c), (d) and (e). (not (f)) . As this layer is rather new compared to previous products I think this should be highlighted (move A6 to the main text ?). Are the front useful in these maps ?

We acknowledge this valuable suggestion. To more clearly represent the observational coverage, our gridding procedure follows a straightforward bin-averaging approach without applying any horizontal interpolation or objective mapping. The scarcity of data in the abyssal layer of Float Grid mainly reflects the limited number of Deep Argo observations currently available at such depths. To better align with our study, which integrates both float- and ship-based observations, we have added the All-Data Grid distributions for the abyssal layer in the main text, providing the most comprehensive observation-based representation below 4,000 m. The frontal lines in the original abyssal-layer maps were included solely for consistency with the maps of other layers and did not serve additional interpretative purposes.

In addition, we have revised Section 4.3 to include the following description for the abyssal layer:

“Figure 9 presents the distributions in the abyssal layer. Because observations below 4,000 m are extremely scarce, the All-Data Grid is used to provide the most comprehensive depiction of deep-ocean conditions.” (Line 384)

“In the deep and abyssal layer (2000-5600 m, Figure 9c), the spatial patterns of DIC and C_{ant} remain unchanged, and their vertical profiles flatten. Both DIC and C_{ant} exhibit relatively high concentrations in the eastern Antarctic region, where Antarctic Bottom Waters (AABW) forms (Morrison et al., 2020). This enrichment is consistent with AABW-driven transport of anthropogenic carbon into the deep ocean.” (Line 404)

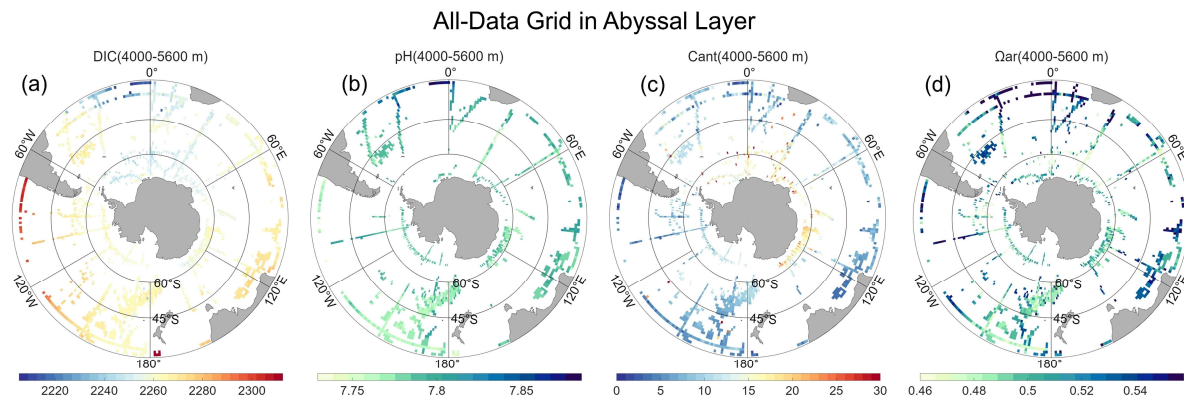


Figure 9. Averaged climatological distribution of DIC (a), C_{ant} (b), pH (c), and Ω_{ar} (d) in the abyssal layer (4000 to 5600 m). The climatology is based on the All-Data Grid combined float- and ship-based observations. Note that the color scales differ among the individual maps.

C-30: Figures A8 and A9: Missing units for these maps.

The missing units have been added to the maps.

;;;;; in references:

C-31: Line 607: Clement and Gruber (2018) not listed in the manuscript.

We have removed the reference.

C-32: Line 656: Change the reference: Lo Monaco C., C. Goyet, N. Metzl, A. Poisson and F. Touratier, 2005. Distribution and inventory of anthropogenic CO₂ in the Southern Ocean : comparison of three data-based methods. *Journal Geophys. Res.* . 110, C09S02, doi:10.1029/2004JC002571.

We have replaced the previous reference (Hauck et al., 2020) with Lo Monaco et al., 2005 (Line 756).

;;;;; Reference added in this review not listed in the Manuscript:

Gruber, N., 1998. Anthropogenic CO₂ in the Atlantic Ocean. *Global Biogeochem. Cycles*, 12, 165–191.

Jiang, L.-Q., et al.,: Synthesis of data products for ocean carbonate chemistry, *Earth Syst. Sci. Data Discuss.* [preprint], <https://doi.org/10.5194/essd-2025-255>, in review, 2025.

Keppler, L., Landschützer, P., Gruber, N., Lauvset, S. K., and Stemmler, I.: Seasonal carbon dynamics in the near-global ocean, *Global Biogeochemical Cycles*, 34(12), e2020GB006571, <https://doi.org/10.1029/2020GB006571>, 2020.

Keppler, L., Landschützer, P., Lauvset, S. K., and Gruber, N.: Recent trends and variability in the oceanic storage of dissolved inorganic carbon, *Global Biogeochemical Cycles*, 37(5), <https://doi.org/10.1029/2022gb007677>, 2023.

Lauvset, S. K, R. M. Key, A. Olsen, S. van Heuven, A. Velo, X. Lin, C. Schirnack, A. Kozyr, T. Tanhua, M. Hoppema, S. Jutterström, R. Steinfeldt, E. Jeansson, M. Ishii, F. F. Pérez, T. Suzuki & S. Watelet, 2016. A new global interior ocean mapped climatology: the 1°x1° GLODAP version 2. *Earth Syst. Sci. Data*, 8, 325-340, doi:10.5194/essd-8-325-2016.

Lo Monaco C., C. Goyet, N. Metzl, A. Poisson and F. Touratier, 2005. Distribution and inventory of anthropogenic CO₂ in the Southern Ocean : comparison of three data-based methods. *Journal Geophys. Res.* . 110, C09S02, doi:10.1029/2004JC002571.

Mahieu, L., Lo Monaco, C., Metzl, N., Fin, J., and Mignon, C.: Variability and stability of anthropogenic CO₂ in Antarctic Bottom Water observed in the Indian sector of the Southern Ocean, 1978–2018, *Ocean Sci.*, 16, 1559–1576, <https://doi.org/10.5194/os-16-1559-2020>, 2020.

Metzl, N., et al: Anthropogenic CO₂, air–sea CO₂ fluxes, and acidification in the Southern Ocean: results from a time-series analysis at station OISO-KERFIX (51° S–68° E), *Ocean Sci.*, 20, 725–758, <https://doi.org/10.5194/os-20-725-2024>, 2024.

Müller, J. D. , N. Gruber, B. Carter, R. Feely, M. Ishii, N. Lange, S. K. Lauvset, A. Murata, A. Olsen, F. F. Pérez, C. Sabine, T. Tanhua, R. Wanninkhof, D. Zhu, Decadal trends in the oceanic storage of anthropogenic carbon from 1994 to 2014. *AGU Adv.* 4, e2023AV000875 (2023).

Orsi, A. H., T. Whitworth III, and W. D. Nowlin Jr., On the meridional extent and fronts of the Antarctic Circumpolar Current, *Deep Sea Res., Part I*, 42, 641-673, 1995.

Pardo, P. C., et al,: Carbon uptake and biogeochemical change in the Southern Ocean, south of Tasmania. *Biogeosciences*, 14(22), 5217–5237. <https://doi.org/10.5194/bg-14-5217-2017>, 2017

Ríos, A. F., Velo, A., Pardo, P. C., Hoppema, M., and Pérez, F. F.: An update of anthropogenic CO₂ storage rates in the western South Atlantic basin and the role of Antarctic Bottom Water, *J. Mar. Syst.*, 94, 197–203, <https://doi.org/10.1016/j.jmarsys.2011.11.023>, 2012.

Rödenbeck, C., et al, 2015. Data-based estimates of the ocean carbon sink variability – First results of the Surface Ocean pCO₂ Mapping intercomparison (SOCOM). *Biogeosciences* 12: 7251-7278. doi:10.5194/bg-12-7251-2015..

Vazquez-Rodriguez, M., et al, 2009. Anthropogenic Carbon Distributions in the Atlantic Ocean: databased estimates from the Arctic to the Antarctic. *Biogeosciences*, 6, 439-451. <https://doi.org/10.5194/bg-6-439-2009>

We sincerely appreciate your careful and constructive review, as well as the inclusion of relevant references that greatly assisted us in refining and improving the manuscript. We carefully reviewed each cited paper and, after evaluating their relevance to our study, made the following adjustments to the reference list and corresponding text:

- (1) Replaced *Zemskova et al., 2022* with *Rios et al., 2012*, *Pardo et al., 2017*, and *Mahieu et al., 2020* (Line 46).
- (2) Added *Lauvset et al., 2016* (Line 68).
- (3) Replaced Hauck et al., 2023 with *Hauck et al., 2023* and *Lo Monaco et al., 2005* (Line 71).
- (4) Added the previously missing references *Zhang et al., 2023* and *Metzl et al., 2024* (Line 104).
- (5) Added *Gruber et al., 1998* (Line 197).
- (6) For citations of the TrOCA method in the Southern Ocean, included *Metzl et al., 2024*; *Vázquez-Rodríguez et al., 2009*; and *Mahieu et al., 2020* (Line 205).
- (7) Updated the CO2SYS reference to *Sharp et al., 2023* (Line 214).
- (8) Added *Orsi et al., 1995* in the caption of Figure 7, 8, A4, A5.